Mathematics and Computers in Simulation XXI (1979) 197–206
North-Holland Publishing Company

SIMULATION OF MAGLEV VEHICLES RIDING OVER SINGLE AND DOUBLE SPAN GUIDEWAYS

Reinhold MEISINGER

Simulation- and Control Department, Spaceflight Division, Messerschmitt-Bölkow-Blohm GmbH, Munich, F.R.G.

A magnetically levitated high speed vehicle on an elevated periodically supported guideway is approximated by a single-mass vehicle on a flexible single and double span beam with rigid piers. To describe the distributed parameter system of the flexible guideway, modal analysis technique is used. Because of the coupling of the moving vehicle and the guideway the system is characterized by an ordinary vector differential equation with periodically time varying coefficients and jumping states at the piers. To compensate the static instability the suspension magnets are actively controlled by a suboptimal time invariant control system. For the single span guideway an analog simulation is shown, whereas for the double span guideway a digital simulation is presented. Examples are given comparing the solutions for dynamic displacements of the system when a direct state feedback controller is used an when the vehicle is modelled as a moving mass or a moving force.

1. INTRODUCTION

In the past few years considerable effort has gone into finding new solutions for fast rail transportation systems [9]. The feasibility of the electromagnetic levitation concept has been proven by test runs in the speed range up to 400 km/h, cf. [4,6]. For economic reasons magnetically levitated vehicles will operate on elevated periodically supported guideways, Fig. 1, which will be light and flexible [8,11]. Because of the instability of the electromagnetic levitation system the vehicle must be actively controlled. Such control concepts have been designed with and without consideration of the guideway flexibility [5,7,8]. The coupled vehicle/guideway system (single span guideway) at high velocities has been simulated using digital computers [10]. An analog simulation [8], however, is necessary if real components of the control system are tested in the closed loop system. In this paper the elastic structure of the guideway is approximated by homogenous elastic single and double span beams described by partial BERNOULLI-EULER beam equations [13]. For typical guideway configurations this approximation is permissible since the lenghts of the beams are large compared with the other dimensions, and these also large compared with the deflections. The investigation of the mass-point vehicle is restricted to motion in vertical plane only, because this motion is influenced by a gravity load and an inertial load. The partial differential equation can be transformed into an infinite number of ordinary differential equations by means of a modal transformation. The kernels of this transformation consist of the eigenfunctions of the force-free beam. An approximation is achieved by considering only the first elements (modes) of the infinite dimensional vector. The mathematical description of the linear time variable system with periodic coefficients and jumping states at the piers is given in state space notation which can be directly used for the digital simulation, cf. [8,11]. In the analog simulation, the fact is used that a linear system with periodic coefficients also may be considered as a nonlinear system with constant coefficients. If the control system synthesis is performed for the vehicle alone, the problem leads to a state feedback controller with constant coefficients. A quadratic criterion is used to optimize the control system. The general control problem includes two limiting cases, cf. [1]. In the first, the magnet gap is constant (moving mass problem) and in the second the magnet force is constant (moving force problem). In the single span case the steady-state responses of the system are found by analog simulation over a great number of periods considering the jumping states at the

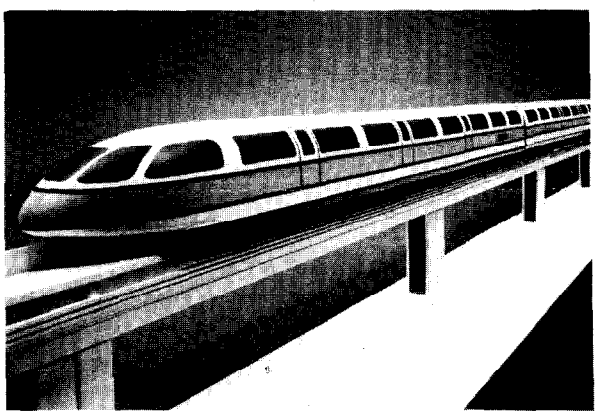

Fig. 1: MAGLEV vehicle on elastic guideway.

piers. In the double span case the system was integrated numerically over an intervall of one period using a 4th order RUNGE-KUTTA algorithm to yield the fundamental matrix. After this only matrix operations where necessary to obtain the steady-state periodic solution of the system. In the examples it is assumed that the static deflection of the elastic guideway by its own weight is compensated.

2. GUIDEWAY MODEL

The guideway is described as a homogenous elastic single and double span beam mounted with pivots on rigid piers. Equations of motions are derived on the basis of BERNOULLI-EULER beam theory, cf. [13].
If l is the length of one span and l_b the length of the beam, the guideway is determined by its first vibration mode frequency f_1 and its span mass m_1. As shown in Fig. 2 the concentrated magnet force, $F(t) = m_f(g-\Delta\ddot{z})$, moves along the span with constant velocity v.

With the nondimensional variables

$$\xi = x/l, \quad \tau = vt/l, \quad \Delta\bar{h}(\xi,\tau) = \Delta h(x,t)/h_{sm},$$

where h_{sm} is the maximum static span deflection of a single span caused from the concentrated weight $m_f g$ of the vehicle, the nondimensional guideway equation of motion is

$$\frac{\partial^2 \Delta\bar{h}(\xi,\tau)}{\partial\tau^2} + \frac{1}{\pi^2\varkappa^2}\frac{\partial^4 \Delta\bar{h}(\xi,\tau)}{\partial\xi^4} = \bar{F}(\tau)\delta(\xi-\tau), \qquad (1)$$

with the 4 boundary and (λ_b-1) intermediate conditions of the beam

$$\Delta\bar{h}(\xi,\tau) = \frac{\partial^2 \Delta\bar{h}(\xi,\tau)}{\partial\xi^2} = 0, \quad \xi = 0,\lambda_b, \qquad (2)$$
$$\Delta h(\xi,\tau) = 0, \quad \xi = 0(1)\lambda_b.$$

In eq. (1) δ is the DIRAC delta function and $F(\tau)$ is the nondimensional magnet force which can be written as

$$\bar{F}(\tau) = \frac{48}{\pi^2\varkappa^2} - \mu\Delta\ddot{\bar{z}}, \qquad \Delta\ddot{\bar{z}} = \frac{(l/v)^2}{h_{sm}}\Delta\ddot{z}. \qquad (3)$$

where $\Delta\ddot{z}$ is the vehicle acceleration.
The system parameters in eq. (1), eq. (2) and eq. (3) are:

$$\varkappa = \frac{v/l}{2f_1}, \quad \mu = m_f/m_1, \quad \lambda_b = l_b/l,$$

where $\varkappa$ is the span crossing frequency ratio, λ the beam to span length ratio and μ the vehicle to span mass ratio.

Modal approximation

Based on the boundary and intermediate conditions of the beam (2), eigenfunctions $\varphi_j(\xi)$, and eigenvalues λ_j can be obtained by solving the eigenvalue problem

$$\frac{1}{\pi^2\varkappa^2}\frac{\partial^4\varphi_j(\xi)}{\partial\xi^4} = -\lambda_j\varphi_j(\xi), \quad j = 1(1)\infty. \qquad (4)$$

With the orthonormality relation

$$\lambda_b\int_0^1 \varphi_j(\xi)\,\varphi_k(\xi)\,d\xi = \delta_{jk} \quad \text{and} \quad \beta_j^4 = -\lambda_j\pi^2\varkappa^2$$

the following results are obtained

a) Eigenfunctions of a single span ($\lambda_b = 1$) and antimetric eigenfunctions of a double span ($\lambda_b = 2$)

$$\varphi_j(\xi) = C_j \sin(\beta_j\xi), \quad j = \begin{cases} 1,2,3.....\text{for } \lambda_b = 1 \\ 1,3,5,....\text{for } \lambda_b = 2 \end{cases}$$

parameter β_j: $\beta_j = (\lambda_b + j - 1)\pi/\lambda_b$,

coefficient C_j: $C_j = \sqrt{2/\lambda_b}$,

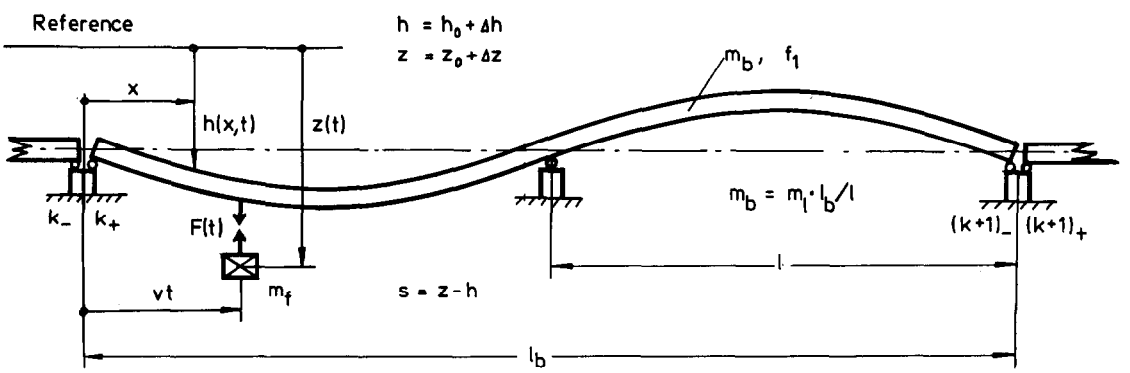

Fig. 2: MAGLEV single mass vehicle on elevated periodically supported double span guideway.

b) Symmetric eigenfunctions of a double span, j = 2,4,6,.....

$$\varphi_j(\xi) = C_j[\cosh(\beta_j)\sin(\beta_j\xi^*) - \cos(\beta_j)\sin(\beta_j\xi^*)]$$

where $\xi^* = \begin{cases} \xi & \text{for } \xi \in [0,1] \\ (2-\xi) & \text{for } \xi \in [1,2] \end{cases}$

parameter β_j	coefficient C_j
$\beta_2 = 3.926602$	$C_2 = 3.942106\ 10^{-2}$
$\beta_4 = 7.068582$	$C_4 = 1.702875\ 10^{-3}$
$\beta_6 = 10.210176$	$C_8 = 7.358789\ 10^{-5}$
$\beta_8 = 13.351768$	$C_8 = 3.180021\ 10^{-6}$
$\beta_{10} = 16.493361$	$C_{10} = 1.374213\ 10^{-7}$
.	.
.	.

When only the first n* eigenfunctions φ_j are considered, it can be shown that an approximation of eq. (1) can be written as, cf. [8,13]

$$\Delta h(\xi,\tau) = \sum_1^{n^*} \varphi_j(\xi)\ \Delta h_j^*(\xi) = \underline{\varphi}(\xi)\ \Delta\underline{h}^*(\tau), \qquad (5)$$

where $\underline{\varphi}$ is the n*x1-vector of the eigenfunctions and Δh^* is the n*x1-vector of the modal coordinates which is obtained as

$$\Delta\ddot{\underline{h}}^* = \underline{\Lambda}\,\Delta\underline{h}^* + \underline{\varphi}(\tau)\left[\frac{48}{\pi^2\alpha^2} - \mu\,\Delta\ddot{\bar{z}}\right], \qquad (6)$$

with the n*xn*-diagonal matrix $\underline{\Lambda} = \mathrm{diag}(\lambda_j)$.

NOTE: Eq. (5) is exact in the case $n^* \to \infty$. For a finite number n* the approximation converges with $(\lambda_b/n^*)^4$. Investigations have shown [8], that for a moving force the result is close enough if approximately $n^* = 2\lambda_b$ eigenfunctions are considered, cf. appendix.

3. VEHICLE MODEL

The single-mass vehicle shown in Fig. 2, with electromagnetic suspension shown in [5, 8], is determined by its mass m_f, the magnet resistance R, the total nominal magnet inductance L_o and the constant magnet stray inductance L_{stray}. The vehicle coordinate system is moving with constant velocity v along the guideway with the span length l.

With the nondimensional variables

$$\Delta\bar{z} = \Delta z/h_{sm}, \quad \tau = vt/l, \quad \Delta\bar{U} = \frac{s_o}{h_{sm}\,U_o}\Delta U,$$

where s_o is the nominal magnet gap, U_o is the nominal magnet voltage and h_{sm} is the maximum static span deflection, the nondimensional linearized vehicle equation of motion is, cf. [8]

$$\Delta\ddot{\bar{z}} = \alpha\beta\Delta\bar{s} + \alpha\eta\Delta\dot{\bar{s}} - \beta\Delta\bar{z} - \alpha\beta\Delta\bar{U}. \qquad (7)$$

Neglecting deterministic and stochastic guideway disturbances the deviation from nominal magnet gap is obtained with eq. (5) as

$$\Delta\bar{s} = \Delta\bar{z} - \underline{\varphi}^T(\tau)\Delta\underline{h}^*. \qquad (8)$$

The system parameters in eq. (7) are:

$$\alpha = \frac{2g}{s_o}\left[\frac{l}{v}\right]^2, \quad \beta = \frac{R}{L_o}\frac{l}{v}, \quad \eta = L_{stray}/L_o,$$

where α, β are nondimensional magnet parameters and η is the stray to total inductance ratio. In case that there is no stray flux ($\eta = 0$) the influence of the magnet gap velocity

$$\Delta\dot{\bar{s}} = \Delta\dot{\bar{z}} - \underline{\varphi}^T(\tau)\ \Delta\dot{\underline{h}}^* - \dot{\underline{\varphi}}^T(\tau)\ \Delta\underline{h}^*$$

becomes zero. A mathematical model for an extended elastic vehicle with continuous magnet distribution is treated in [8].

4. VEHICLE/GUIDEWAY MODEL

The mathematical description of the open-loop vehicle/guideway system depends on the subsystems described in eq. (6) and eq. (7). For the further treatment it is assumed, that the following signals can be measured by sensors [1]:

$\Delta\bar{s}(\tau)$ = magnet gap,
$\Delta\dot{\bar{s}}(\tau)$ = magnet gap velocity,
$\Delta\ddot{\bar{z}}(\tau)$ = vehicle acceleration.

The assumption, that the magnet gap velocity is available will be realized in practive by an observer which gives an optimal estimation of $\Delta\dot{\bar{s}}(\tau)$, cf. [8]. Introducing the state space notation the system can be written as shown in eq. (9) with the nx1-state vector $\underline{x}$, (n = 3+2n*), the periodic nxn-system matrix $\underline{A}(\tau) = \underline{A}(\tau+\lambda_b)$ the nx1-input matrix $\underline{D}$, the periodic nx1-disturbance matrix $\underline{B}(\tau) = \underline{B}(\tau+\lambda_b)$, the periodic 3xn-measurement matrix $\underline{C}(\tau) = \underline{C}(\tau+\lambda_b)$, the nxn-jumping matrix $\underline{\Gamma}$, the 3x1-measurements vector $\underline{y}$, the scalar input u and the scalar disturbance signal b.

The matrix $\underline{\Gamma}$ considers that the guideway states are jumping if the vehicle leaves the beam at time $\tau = k\lambda_b$.

$$\Delta h_{k+}^* = \Delta\dot{h}_{k+}^* = 0, \quad k = 0,1,2,.....$$

Because of the coupling between the moving vehicle and the guideway the linear system (9) can be characterized as periodically time varying with jumping states.

---

[1] The dynamics of the sensors is neglected in the equations.

$$
\left.
\begin{aligned}
&\text{vehicle}\\
&\text{guideway}
\end{aligned}
\left\{
\begin{bmatrix} \Delta\dot{z} \\ \Delta\ddot{z} \\ \Delta\dddot{z} \\ \Delta\dot{\underline{h}}^{*} \\ \Delta\ddot{\underline{h}}^{*} \end{bmatrix}
=
\left[\begin{array}{ccc|cc}
0 & 1 & 0 & \underline{0} & \underline{0} \\
0 & 0 & 1 & \underline{0} & \underline{0} \\
\alpha\beta & \alpha\eta & -\beta & -\alpha(\beta\varphi^{T}+\eta\dot{\varphi}^{T}) & -\alpha\eta\varphi^{T} \\
\hline
\underline{0} & \underline{0} & \underline{0} & \underline{0} & \underline{E} \\
\underline{0} & \underline{0} & -\mu\underline{\varphi} & \underline{\Lambda} & \underline{0}
\end{array}\right]
\begin{bmatrix} \Delta z \\ \Delta\dot{z} \\ \Delta\ddot{z} \\ \Delta\underline{h}^{*} \\ \Delta\dot{\underline{h}}^{*} \end{bmatrix}
+
\begin{bmatrix} 0 \\ 0 \\ -\alpha\beta \\ \underline{0} \\ \underline{0} \end{bmatrix}
\Delta\bar{U}
+
\begin{bmatrix} 0 \\ 0 \\ 0 \\ \underline{0} \\ \underline{\varphi} \end{bmatrix}
\frac{48}{\pi^{2}\varkappa^{2}},
\right.
$$

$$
\underbrace{\dot{\underline{x}}}_{} = \underbrace{\underline{A}(\tau)}_{} \cdot \underbrace{\underline{x}}_{} + \underbrace{\underline{D}\cdot u}_{} + \underbrace{\underline{B}(\tau)\cdot b}_{}
$$

$$
\left.
\begin{aligned}
&\text{measure-}\\
&\text{ments}
\end{aligned}
\left\{
\begin{bmatrix} \Delta\bar{s} \\ \Delta\dot{\bar{s}} \\ \Delta\ddot{\bar{z}} \end{bmatrix}
=
\left[\begin{array}{ccc|cc}
1 & 0 & 0 & -\varphi^{T} & \underline{0} \\
0 & 1 & 0 & -\dot{\varphi}^{T} & -\varphi^{T} \\
0 & 0 & 1 & \underline{0} & \underline{0}
\end{array}\right]
\begin{bmatrix} \Delta\bar{z} \\ \Delta\dot{\bar{z}} \\ \Delta\ddot{\bar{z}} \\ \Delta\underline{h}^{*} \\ \Delta\dot{\underline{h}}^{*} \end{bmatrix},
\qquad
\begin{bmatrix} \Delta z \\ \Delta\dot{z} \\ \Delta\ddot{z} \\ \Delta\underline{h}^{*} \\ \Delta\dot{\underline{h}}^{*} \end{bmatrix}_{k+}
=
\left[\begin{array}{ccc|cc}
1 & 0 & 0 & \underline{0} & \underline{0} \\
0 & 1 & 0 & \underline{0} & \underline{0} \\
0 & 0 & 1 & \underline{0} & \underline{0} \\
\hline
\underline{0} & \underline{0} & \underline{0} & \underline{0} & \underline{0} \\
\underline{0} & \underline{0} & \underline{0} & \underline{0} & \underline{0}
\end{array}\right]
\begin{bmatrix} \Delta\bar{z} \\ \Delta\dot{\bar{z}} \\ \Delta\ddot{\bar{z}} \\ \Delta\underline{h}^{*} \\ \Delta\dot{\underline{h}}^{*} \end{bmatrix}_{k-}.
\right.
\qquad (9)
$$

$$
\underbrace{\underline{y}}_{} = \underbrace{\underline{C}(\tau)}_{} \cdot \underbrace{\underline{x}}_{}, \qquad \underbrace{\underline{x}_{k+}}_{} = \underbrace{\underline{\Gamma}}_{} \cdot \underbrace{\underline{x}_{k-}}_{}
$$

5. CONTROLLER WITH CONSTANT COEFFICIENTS

To compensate the static instability of the magnetically levitated vehicle, the suspension magnets have to be actively controlled. When the guideway is neglected, or a rigid straight-line guideway is assumed, the vehicle motion alone can be described with the linear time invariant 3rd order system

$$\dot{\underline{x}}_f = \underline{A}_f\,\underline{x}_f + \underline{D}_f\,u, \qquad \underline{y} = \underline{x}_f, \qquad (10)$$

where $\underline{x}_f$ is the 3×1-state vector, $\underline{y}$ the 3×1-measurement vector, u the scalar input signal and $\underline{A}_f$, $\underline{D}_f$ are matrices of order compatible with the relating vectors.
For the design of an suboptimal state feedback controller several techniques can be used, such as quadratic loss criterions and arbitrary dynamic algorithms, cf. [5]. If the conditions of controllability are satisfied [2], the linear time invariant control law

$$u = -\underline{K}_f\,\underline{y} \qquad (11)$$

is sufficient to stabilize the vehicle.
Here the quadratic loss criterion

$$I = \frac{1}{2}\int_0^{\infty}\left[\underline{x}_f\,\underline{G}\,\underline{x}_f + H\,u^2\right]\mathrm{d}\tau \qquad (12)$$

is used to optimize the system (10), cf. [2]. If the state components are weighted by the 3×3-matrix $\underline{G} = \mathrm{diag}\,[G_i]$, i = 1(1)3, and the input signal by the scalar quantity H, the 3×1-feedback matrix $\underline{K}_f$ in eq. (11) can be written as

$$\underline{K}_f = \underline{D}_f\,\underline{P}_f/H, \qquad (13)$$

where the 3×3-matrix $\underline{P}_f$ is obtained as a solution of the algebraic matrix RICCATI-equation

$$\underline{P}_f\underline{A}_f + \underline{A}_f^{T}\,\underline{P}_f + \underline{G} - \underline{P}_f\underline{D}_f\underline{K}_f = \underline{0}. \qquad (14)$$

This equation can be solved numerically with POTTERS algorithm [12].
If the guideway states are included in the control system design an optimal controller with steady state periodic coefficients is obtained, cf. [7,8]. Then the corresponding matrix RICCATI-equation is also periodic.

6. DIGITAL AND ANALOG SIMULATION

To yield the steady-state solution of the problem the state equation for the controlled system

$$\dot{\underline{x}} = \left[\underline{A}(\tau) - \underline{D}\underline{K}_f\underline{C}(\tau)\right]\underline{x} + \underline{B}(\tau)\,b, \qquad (15)$$

cf. eq. (9) and eq. (11) can be integrated with an analog computer over a great number of periods considering the jumping states.
The same result is obtained numerically with the following equation

$$\underline{x}_{\infty+} = \left[\underline{E} - \underline{\Gamma}\,\underline{\Phi}(\lambda_b)\right]^{-1}\underline{\Gamma}\,\underline{B}^{*}b, \qquad (16)$$

where $\underline{x}_{\infty-}$ is the steady-state solution of eq. (15) at time $\tau = (k\lambda_b + 0)$ and $\underline{\Phi}(\lambda_b)$ is the n×n-fundamentalmatrix of eq. (15), which can be solved by integration of the differential equation

$$\dot{\underline{\Phi}}(\tau) = \left[\underline{A}(\tau) - \underline{D}\underline{K}_f\underline{C}(\tau)\right]\underline{\Phi}(\tau), \quad \underline{\Phi}(0) = \underline{E}, \qquad (17)$$

over one period, and $\underline{B}^{*}$ is the 3×1-Matrix

$$\underline{B}^{*} = \int_0^{\lambda_b}\underline{\Phi}(\lambda_b,\tau)\,\underline{B}(\tau)\,\mathrm{d}\tau.$$

The advantage of analog simulation technique is that real components of the controller can be tested in the closed loop system. Within the analog simulation the fact is used, that the time-variable linear system (15) with periodic coefficients also may be considered as a nonlinear System with constant coefficients. The simulation in the main then only requires the generation of the eigenfunctions, as well as the performance of fourier-analysis and fourier-synthesis, cf. circuit diagram in Fig. 3. Because of the concentrated load at $\xi = \tau$ the fourier-analysis reduces to a multiplication of the modal coordinate $\Delta h_j^{*}(\tau)$ with the eigenfunction $\varphi_j(\xi{=}\tau)$. The fourier-synthesis (Integration

along the spatial coordinate $\xi = \tau$) however is carried out in high-speed repetitive mode (IC-OPERATE with $\tau^* = 0{,}001\,\tau$), as the only independent variable at the analog computer is the time τ, [3]. Therefore $\Delta h_j^*(\tau)$ has to be multiplied with $\varphi_j(\xi=\tau)$ and then added together. The multiplication is done in such a manner, that the amplitudes of the spatial profile are used as initial condition for the integration. Because of the high computation frequency, the result $\Delta\bar{h}(\tau^*,\tau)$, shown on an analog video display, gives the impression of continuously changing spatial profiles. If only the deflection under the load is of interest, the fourier-synthesis reduces to the multiplication of $\Delta h_j^*(\tau)$ with $\varphi_j(\xi=\tau)$. The integration over a great number of periods is carried out in repetitive mode (IC-OPERATE at time $\tau = 1$) with guideway initial conditions zero and steady vehicle state components (realized with a resolver).

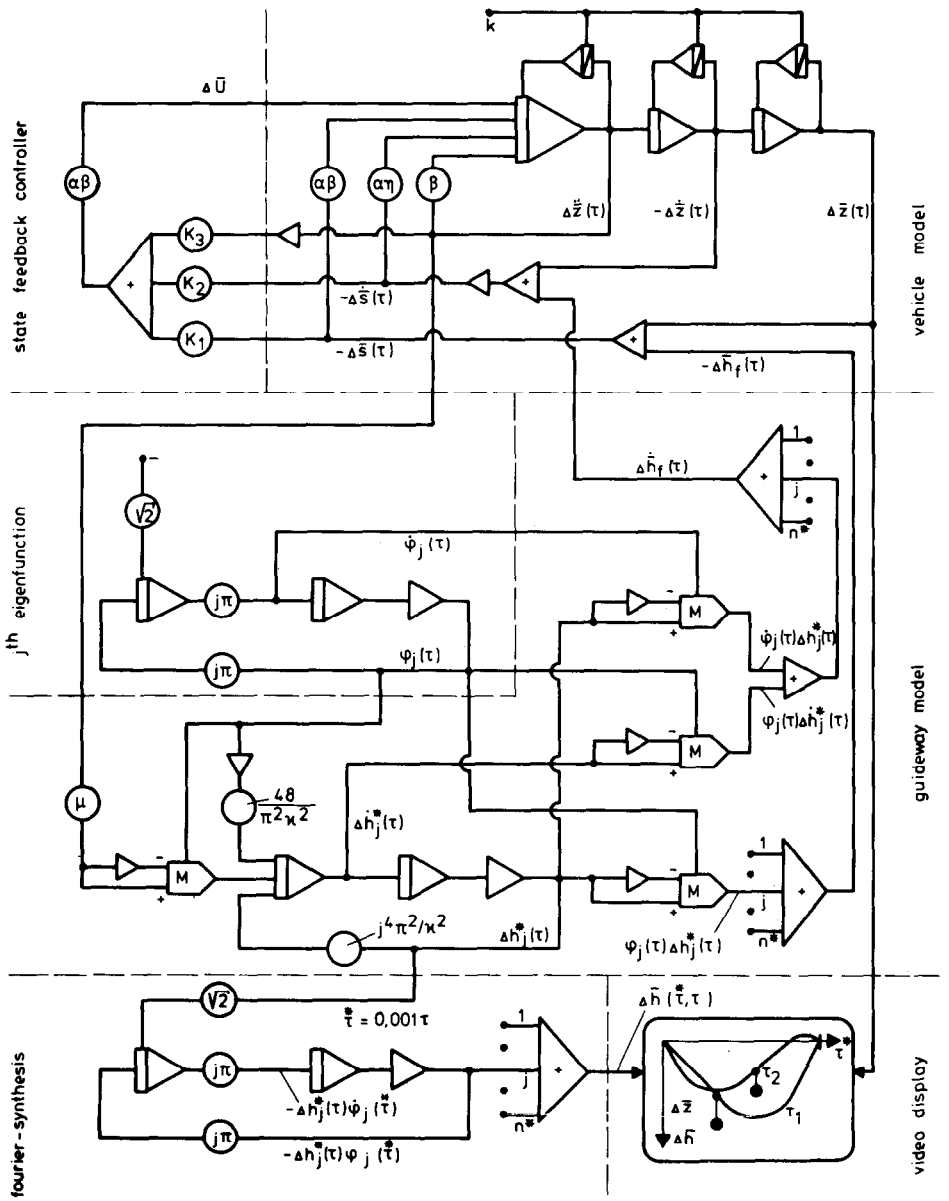

Fig. 3: Circuit diagram for a single mass vehicle on a single span guideway with constant state feedback controller. In the diagram only the generation of the j^{th} eigenfunction is shown.

7. SIMULATION RESULTS

The nondimensional system parameters and controller weightings used for the simulation are (for a span crossing frequency v/l = 6 Hz):

vehicle: $\alpha = 1000/36$, $\beta = 2/3$, $\eta = 0.3$.

The corresponding quantities for the nominal magnet gap s_0, the magnet resistance R and the nominal magnet inductance L_0 are: $s_0 \approx 20$ mm, $R = 2.4\Omega$, $L_0 = 0.6$ H.

guideway: $\varkappa = 0.75$, $\mu = 0.5$.

The guideway used to get this set of parameters are rather flexible having first vibration mode frequencies $f_1 = 4$ Hz.

controller: $\underline{G} = \mathrm{diag}[4\cdot10^4,\ 0,\ 6^4]$, $H = 10^3$.

To demonstrate an approximation of the moving mass problem, cf. appendix, the gap weighting $G_1 = 4\cdot10^4$ is replaced by the quantity $G_1 = 10^8$ for the single span and $G_1 = 10^7$ for the double span guideway.

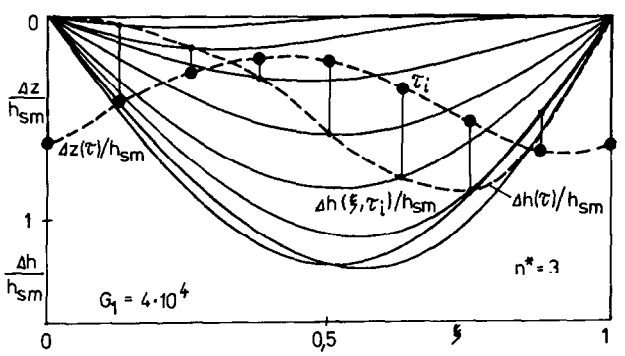

Fig. 4: Spatial single span guideway profiles, histories of vehicle displacement, and single span deflection.

The nondimensional controller-gains K_1, K_2, K_3, which are elements of the 3×1-feedback matrix $\underline{K}_f$, are computed according to eq. (13).

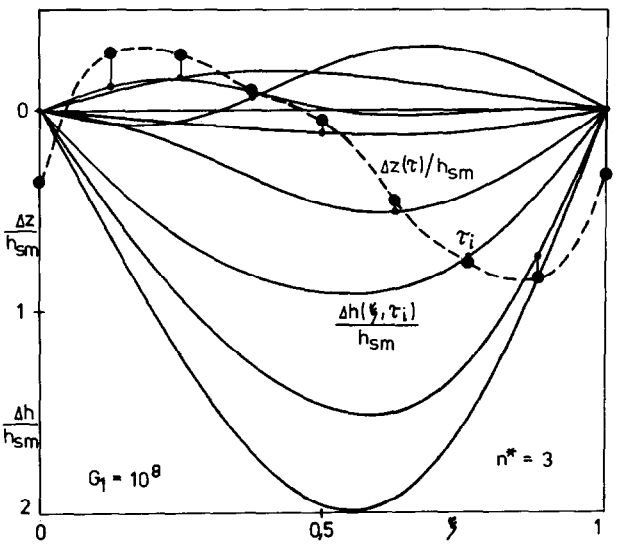

Fig. 5: Spatial single span guideway profiles and histories of vehicle displacement.

Fig. 4 - 5 present the spatial guideway profiles for various locations of the single mass vehicle on a single span guideway for weak ($G_1 = 4\cdot10^4$) and strong ($G_1 = 10^8$) gap weightings. With dotted lines the histories of vehicle displacement and span deflection under the vehicle are shown. In practive the strong weighting of the magnet gap ($G_1 = 10^8$) cannot be realized with an electro magnetic suspension shown in Fig. 3, because this system can generate only tension forces.

Fig. 6 - 7 show the histories of double span deflection under the single mass vehicle, vehicle displacement, vehicle acceleration and

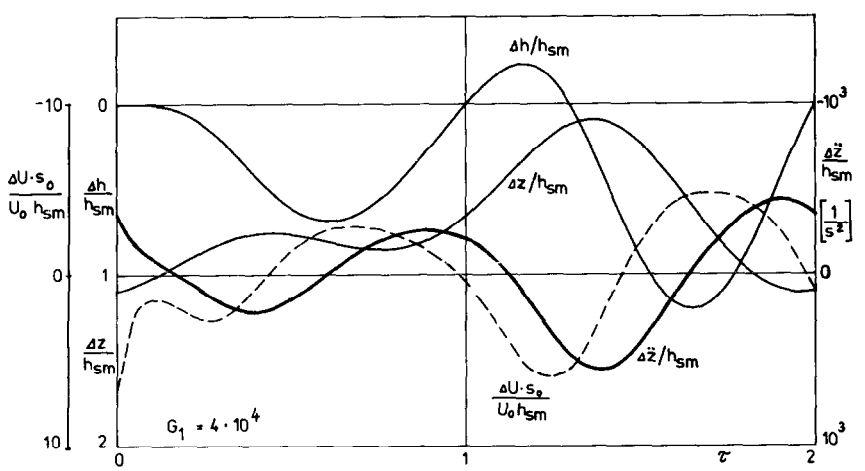

Fig. 6: Histories of double span deflection under the single mass vehicle, vehicle displacement, vehicle acceleration and magnet voltage.

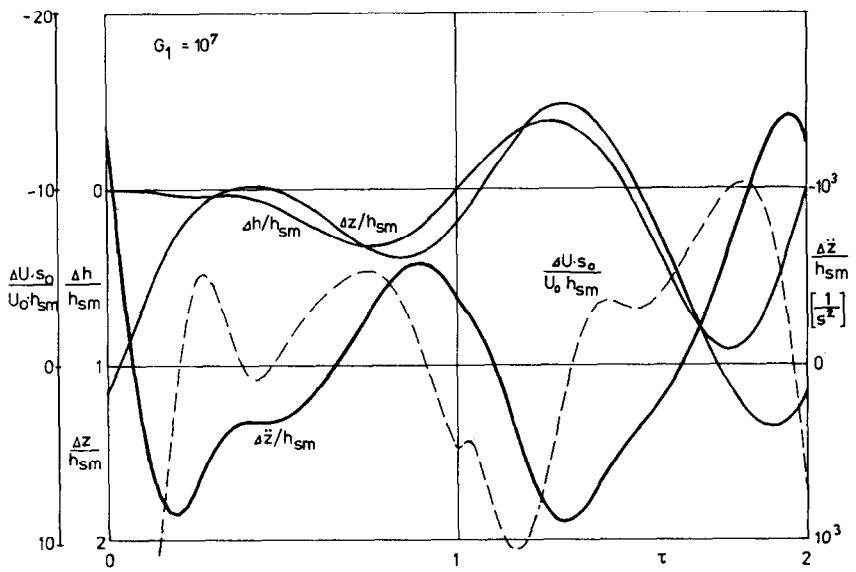

Fig. 7: Histories of double span deflection under the single mass vehicle, vehicle displacement, vehicle acceleration and magnet voltage.

magnet voltage for weak ($G_1 = 4 \cdot 10^4$) and strong ($G_1 = 10^7$) gap weightings.

The analog simulation of the single span system was implemented on the analog computer EAI PACER 231 R, whereas the digital simulation was carried out on a SEL 320 computer.

8. CONCLUSION

In this paper modal analysis techniques has been applied to obtain the state equation of a moving single mass vehicle on a single span guideway. It is possible to stabilize the system with a suboptimal time invariant controller. The conflicting requirements of small magnet gap and passenger comfort however cannot be satisfied without a two body vehicle and secondary suspension, because reducing of vehicle acceleration gives an increase of magnet gap. The simulation results are closely enough if $n^* = 2\lambda_b$ eigenfunctions are considered. With a sufficiently high computation frequency by the analog integration along the spatial profile, the results shown on a display, give the impression of continuously changing profiles. In the case that the generation of the eigenfunctions on the analog computer is to difficult (double span guideway system) a digital simulation is recommendable. In this paper only steady state simulations are demonstrated although the investigations have shown that the transient values of vehicle acceleration and magnet gap are sometimes higher. The simple example of a single mass vehicle has shown, that the elastic guideway must be included in the simulation. The method of approach can be easily extended to the heave-pitch motion and lateral-yaw motion of the vehicle, respectively.

APPENDIX

MOVING MASS AND MOVING FORCE

The general control and simulation problem shown in chapter 5 and chapter 6, includes two closely related problems, both of which are, in a sense, limiting cases.
In the first case, the magnet gap is constant (moving mass problem or ideal s-control) and the vehicle acceleration $\Delta\ddot{z}$ in the righthand side of eq. (6) can be written as, cf. eq. (5).

$$\Delta\ddot{z} = \Delta\ddot{h}(\zeta=\tau) = \underline{\ddot{\varphi}}^T(\tau)\Delta\underline{h}^* + 2\underline{\dot{\varphi}}^T(\tau)\Delta\dot{\underline{h}}^* + \underline{\varphi}^T(\tau)\Delta\ddot{\underline{h}}^* . \quad (A1)$$

In the second case, the magnet force is constant (moving force problem or ideal z-control) and the vehicle acceleration $\Delta\ddot{z}$ in the righthand side of eq. (6) is zero.
With the moving mass acceleration from eq. (A1), the guideway equation (6) can be written as

$$\Delta\ddot{\underline{h}}^* = \underline{I}\underline{\Lambda}^*\Delta\underline{h}^* - 2\mu\underline{I}\underline{\varphi}(\tau)\dot{\underline{\varphi}}^T(\tau)\Delta\dot{\underline{h}}^* + \underline{I}\underline{\varphi}(\tau)\frac{48}{\pi^2\alpha^2} , \quad (A2)$$

where $\underline{I} = [\underline{E} + \mu\underline{\varphi}(\tau)\underline{\varphi}^T(\tau)]^{-1}$,
$\underline{\Lambda}^* = [\underline{\Lambda} - \mu\underline{\varphi}(\tau)\ddot{\underline{\varphi}}^T(\tau)]$
are n×n-matrizes. This time variable equation with periodic coefficients can be integrated numerically with a 4^{th} order RUNGE-KUTTA algorithm over one period, cf. [8].
For the single span system an analog simulation is shown. The circuit diagram for the moving mass, Fig. A1, is of the same form as that for the controlled force case, Fig. 3, except that the vehicle acceleration $\Delta\ddot{z}$ is given by eq. (A1). The algebraic loop in the analog simulation is stabilized with a 1 pF capacitor, cf. Fig. A1.

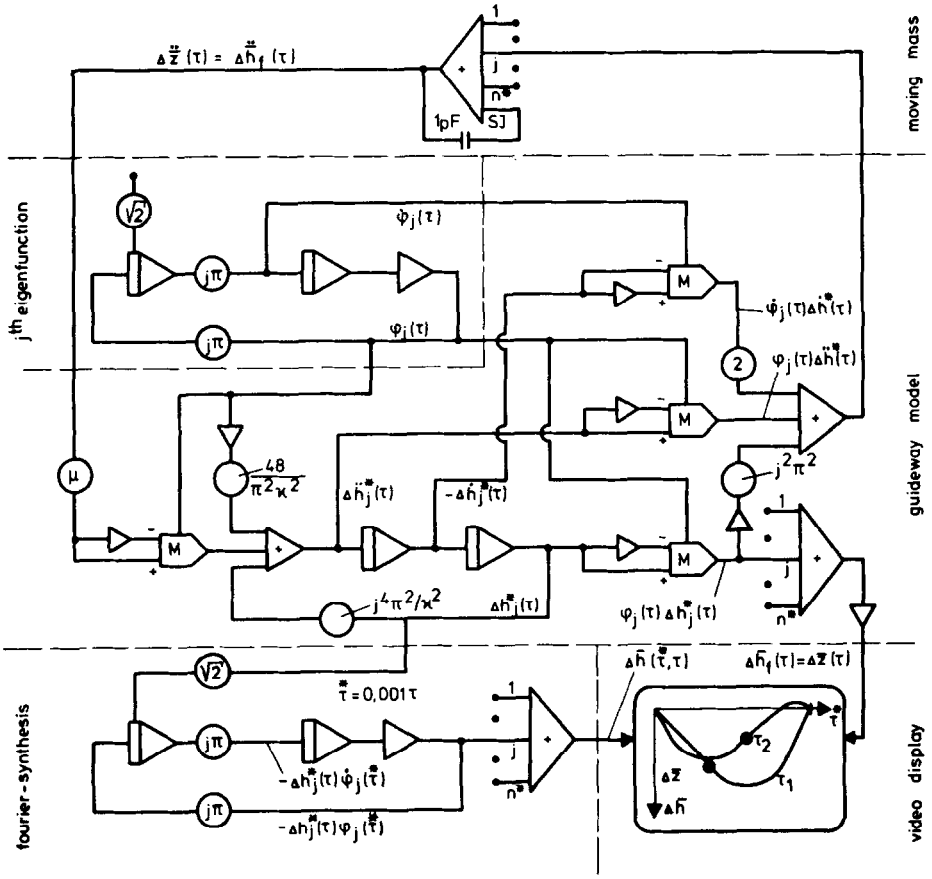

Fig. A1: Circuit diagram for a moving single mass ($\mu \neq 0$) and a moving single force ($\mu = 0$) on a single span guideway. In the diagram only the generation of the j^{th} eigenfunction is shown.

Fig. A2 - A3 illustrate the influence of span crossing frequency ratio $\varkappa$ on the deflection of a single span guideway under a moving single force ($\mu = 0$, ideal z-control) and under a moving single mass (ideal s-control).

Fig. A4 - A5 show the same results for a double span guideway.

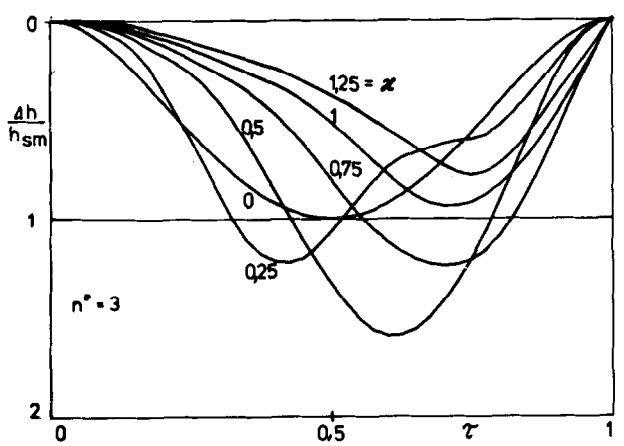

Fig. A2: Histories of single span deflection under a moving single force.

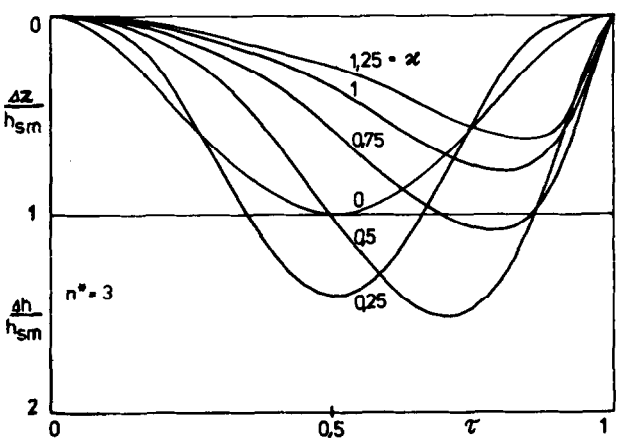

Fig. A3: Histories of single span deflection under a moving single mass ($\mu = 0.5$).

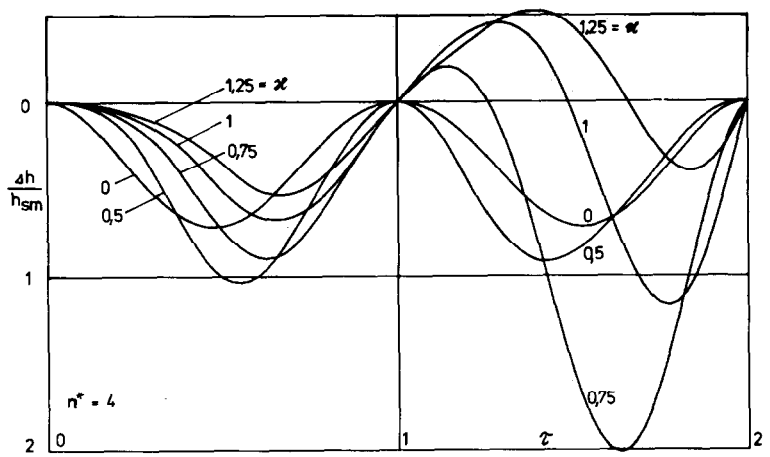

Fig. A4: Histories of double span deflection under a moving single force.

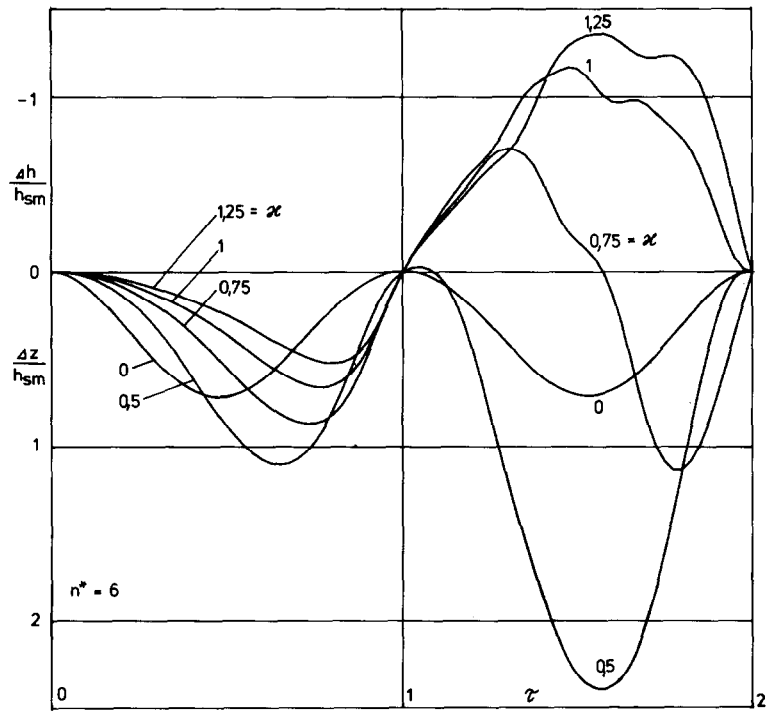

Fig. A5: Histories of double span deflection under a moving single mass (μ = 0.5).

Table A1 presents for a moving single mass on a single and double span guideway the influence of the number n* of eigenfunctions which are considered in the modal approximation and the influence of the vehicle to span mass ratio μ on the exactness of the maximum span deflection solution

$$\Delta h_{max} = \max_{\tau} \left\{ \Delta \bar{h}(\xi = \tau) \right\} .$$

The results show, that for an increasing vehicle to span mass ratio an increasing number n* of eigenfunctions is sufficient to obtain convergence of the approximation.
But for practical purposes the simulation results are closely enough if $n^* = 2\lambda_b$ eigenfunctions are considered. If the static deflection $\Delta h_{max} = h_{sm}$ of a single span is computed using only the first mode it is within 2 percent of the exact static deflection

$$h_{sm} = m_f g l^3/(48\ EI),$$

where EI is the stiffness of the beam, g is the gavitational acceleration, m_f is the vehicle mass and l is the span length.

	$\lambda_b = 1$		$\lambda_b = 2$	
μ	0	0.5	0	0.5
$n^* = \lambda_b$	1.19	0.96	2.00	1.49
$n^* = 2\lambda_b$	1.23	1.07	2.03	1.18
$n^* = 3\lambda_b$	1.24	1.08	2.04	1.14
$n^* = 4\lambda_b$	1.24	1.09	2.04	1.15
$n^* = 5\lambda_b$	1.24	1.09	2.04	1.16

Table A1: Influence of n^* and μ on Δh_{max} for $\varkappa = 0.75$.

ACKNOWLEDGEMENTS

The author gratefully acknowledges the useful advice of Mrs. E. GOTTZEIN, Manager of the Simulation and Control Department, and the support of Mr. K.H. BROCK in analog programming.
The work has been performed under contract of the Ministry of Research and Technology of the Government of the Federal Republic of Germany.

REFERENCES

[1] AYRE, R.S., JACOBSEN, L.S., HSU, C.S.: Transverse Vibration of One and Two-Span Beams under Action of a Moving Mass Load. Proc. of the First U.S. National Congress of Appl. Mech., 1951.

[2] BRYSON, A.E., YU-CHI HO: Applied Optimal Control. Blaisdell Publishing Company, Waltham, Massachusetts, Toronto, London, 1969.

[3] GILLES, E.D., ZEITZ, M.: Modales Simulationsverfahren für Systeme mit örtlich verteilten Parametern. Regelungstechnik, Heft 5 (1969) S. 204-212.

[4] GOTTZEIN, E., BROCK, K.H., SCHNEIDER, E., PFEFFERL, J.: Control Aspects of a Magnetic Levitation High Speed Test Vehicle. Automatica, Vol. 13 (1977) pp. 201-223.

[5] GOTTZEIN, E., LANGE, B.O.: Magnetic Suspension Control Systems for the MBB High Speed Train. Automatica, Vol. 11 (1975) pp. 271-284.

[6] GOTTZEIN, E., MILLER, L., MEISINGER, R.: Magnetic Suspension Control System for High Speed Ground Transportation Vehicles. Proc. of the World Electrotechnical Congress, Moscow, 1977.

[7] MEISINGER, R.: Control Systems for Flexible MAGLEV Vehicles Riding over Flexible Guideways. Proc. of IUTAM Symposium on the Dynamics of Vehicles on Roads and Railway Tracks, Delft, 1975.

[8] MEISINGER, R.: Beiträge zur Regelung einer Magnetschwebebahn auf elastischem Fahrweg. Dr.-Ing. Dissertation, TU München, 1977.

[9] MUCKLI, W.: Bahnsysteme mit berührungsfreier Fahrtechnik. ZEV-Glasers Annalen 100, Nr. 1 (1976) S. 16-19.

[10] POPP, K., HABECK, R., BREINL, W.: Untersuchungen zur Dynamik von Magnetschwebefahrzeugen auf elastischen Fahrwegen. Ingenieur-Archiv 46 (1977) S. 1-19.

[11] POPP, K., SCHIEHLEN, W.: Dynamics of Magnetically Levitated Vehicles on Flexible Guideways. Proc. of the IUTAM Symposium on the Dynamics of Vehicles on Roads and Railway Tracks, Delft, 1975.

[12] POTTER, J.E.: Matrix Quadratic Solutions. SIAM Jour. Appl. Math. Vol. 14 (1966) pp. 496-501.

[13] SZABO, I.: Höhere Technische Mechanik. Springer-Verlag, Berlin, Göttingen, 1956.